of our solutions. For this reason, all of the quantitative WGA studies were done with ferritin-conjugated lectins. Qualitatively similar results were observed with horseradish peroxidase–conjugated WGA.
17. Y. Hu, A. Barzilai, E. R. Kandel, in preparation.
18. R. G. Anderson, M. S. Brown, U. Beisiegel, J. L. Goldstein, *J. Cell Biol.* **93**, 523 (1982).
19. C. Watts, *ibid.* **100**, 633 (1985).
20. D. A. Wall and A. L. Hubbard, *ibid.* **90**, 687 (1981).
21. I. S. Trowbridge, *Curr. Opin. Cell Biol.* **3**, 634 (1991).
22. H. Krämer, R. L. Cagan, S. L. Zipursky, *Nature* **352**, 207 (1991).
23. R. M. Steinman, I. S. Mellman, W. A. Muller, Z. A. Cohn, *J. Cell Biol.* **96**, 1 (1983); J. Gruenberg and K. Howell, *Annu. Rev. Cell Biol.* **5**, 453 (1989); W. Huttner and C. Dotti, *Curr. Opin. Neurobiol.* 1, 388 (1991).
24. For review see [S. Kornfeld and I. Mellman, *Annu. Rev. Cell Biol.* **5**, 483 (1989); F. R. Maxfield and D. J. Yamashiro, in *Acidification of Organelles and the Intracellular Sorting of Proteins during Endocytosis*, C. J. Steer and J. A. Hanover, Eds. (Cambridge Univ. Press, Cambridge, U.K., 1991), pp. 157–182].
25. A total of 13 CURLs from control cells and 56 CURLs from 5-HT–treated cells were analyzed.
26. A. Sheppard, J. Wu, U. Rutishauser, G. Lynch, *Biochim. Biophys. Acta* **1076**, 156 (1991); J. Covault, Q. Y. Liu, S. el-Deeb, *Mol. Brain Res.* 11, 11 (1991).
27. C. H. Bailey, P. G. Montarolo, M. Chen, E. R. Kandel, S. Schacher, in preparation.
28. A. Bretscher, *J. Cell Biol.* **108**, 921 (1989); C. Y. Dadabay, E. Patton, J. A. Cooper, L. J. Pike, *ibid.* **112**, 1151 (1991).
29. J. L. Connolly, S. A. Green, L. A. Green, *ibid.* **98**, 457 (1984); J. L. Connolly, P. J. Seeley, L. A. Greene, *J. Neurosci. Res.* **13**, 183 (1985).
30. P. A. Johnston *et al.*, *EMBO J.* **8**, 2863 (1989).
31. K. H. Pfenninger, in *Axoplasmic Transport in Physiology and Pathology*, D. G. Weiss and A. Gorio, Eds. (Springer-Verlag, Berlin, 1982), pp. 52–61; T. P. O. Cheng and T. S. Reese, *J. Cell Biol.* **101**, 1473 (1985).
32. We thank R. Axel, T. Jessell, F. Maxfield, M. Mayford, and S. Schacher for critical reading of the manuscript; H. Ayers and A. Krawetz for typing the manuscript; and S. Mack for preparation of Fig. 5. Supported by MH37134 from the National Institute of Mental Health, GM32099 from the National Institute of General Medical Sciences, and the McKnight Endowment Fund for Neuroscience to C.H.B., Stiftung für medizinisch-biologische Stipendion (Basel) to F.K., and the Howard Hughes Medical Institute (E.R.K. and F.K.).

26 November 1991; accepted 1 April 1992

Colloid Formation During Waste Form Reaction: Implications for Nuclear Waste Disposal

J. K. Bates, J. P. Bradley, A. Teetsov, C. R. Bradley, M. Buchholtz ten Brink

Insoluble plutonium- and americium-bearing colloidal particles formed during simulated weathering of a high-level nuclear waste glass. Nearly 100 percent of the total plutonium and americium in test ground water was concentrated in these submicrometer particles. These results indicate that models of actinide mobility and repository integrity, which assume complete solubility of actinides in ground water, underestimate the potential for radionuclide release into the environment. A colloid-trapping mechanism may be necessary for a waste repository to meet long-term performance specifications.

Recent emphasis in the U.S. high-level nuclear waste disposal program has focused on determination of the suitability of the potential site at Yucca Mountain, Nevada (*1*). The current reference design (*2*) calls for spent nuclear fuel from commercial reactors and for high-level waste glass to be contained in an engineered barrier system (EBS) that is surrounded by the natural host rock. Ideally, this multiple barrier system (waste form, EBS, rock) limits radionuclide release from the waste material and retard radionuclide migration due to chemical and physical interactions with the rock.

Evaluation of the total system performance has been based on the premise that the release of actinides [for example, Pu and Am (*3*)] from the waste form will be controlled by the solubility of individual elements in ground water and that subsequent radionuclide transport will be determined by factors such as water flow and by radionuclide retardation processes such as sorption (*4–7*). Under this scenario, the waste form itself can react relatively rapidly, yet the transport of radionuclides will be limited by geohydrologic factors.

In this report we demonstrate limitations of the solubility-controlled assumption by examining the release of Np, Pu, and Am from waste glass under simulated storage conditions. Although it is known that radionuclides may form colloids (*8*) that could affect transport properties (*9*, *10*), it has generally been assumed that colloids result from hydrolysis of dissolved species in solution (radiocolloids) or from adsorption of dissolved radionuclides onto suspended mineral particles in the ground water (pseudocolloids) (*5–7*). Both of these processes of colloid formation occur independently of waste form and EBS, and they may be considered secondary processes. However, because glass is a metastable solid, it may transform into a more stable phase assemblage under repository storage conditions (*11*, *12*). This assemblage may be a new source of colloidal material, termed primary colloids, and forms by a process that is dependent on the waste form. The radionuclide content, the sources, and the mechanism of formation of these colloids must be accurately known to assess transport of radionuclides from the EBS to the accessible environment.

Glass may be exposed to a variety of

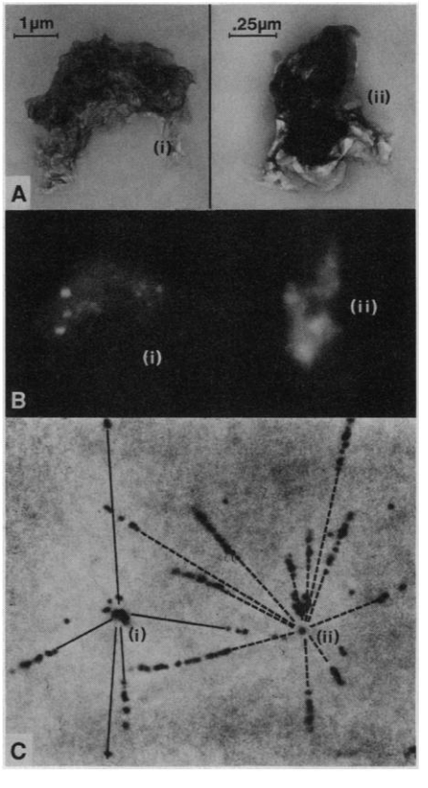

Fig. 1. (**A**) Bright-field electron micrographs of two colloid (residue) particles [labeled (i) and (ii)]. (**B**) Corresponding backscattered electron images. Bright areas indicate high concentrations of brockite (ideally Ca-Th phosphate). (A) and (B) demonstrate that particle (i) contains mostly clay with minor brockite, whereas particle (ii) contains predominantly brockite. (**C**) The α-tracks in nuclear emulsion (with extrapolated trajectories) superimposed on a bright-field image of particles (i) and (ii). The smaller particle, (ii), contains more (Pu- and Am-bearing) brockite and therefore produces more tracks.

J. K. Bates and C. R. Bradley, Argonne National Laboratory, 9700 South Cass Avenue, Argonne, IL 60439.
J. P. Bradley, MVA Incorporated, 5500 Oakbrook Parkway, No. 200, Norcross, GA 30093.
A. Teetsov, McCrone Associates, Incorporated, 850 Pasquinelli Drive, Westmont, IL 60559.
M. B. ten Brink, Lawrence Livermore National Laboratory, Post Office Box 808, Livermore, CA 94550.

conditions after disposal in a geologic repository because the EBS environment changes as the waste cools. For example, at the potential Yucca Mountain site, depending on when the outer containment barrier is breached, glass may be contacted by water vapor, small amounts of sorbed liquid water, or small amounts of flowing water if water enters and trickles through the metal container (*2*). A test method developed to simulate these conditions (*13*) has been applied to a prototype glass (*14, 15*). The method involves dripping water onto a cylindrically shaped glass-metal assemblage that is suspended in an enclosed test vessel. The water flows over the glass, collects at the base, and drips from the assemblage at a rate of about 5 ml per year (one drop every 1 to 2 weeks). Water that collects in the bottom of the test vessel provides information about the form of the radionuclides, the rate by which they are released from the glass, and the synergistic effects that occur in the glass-metal-water system. Such tests have been ongoing for 50 months.

During the most recent liquid collection period, the test solution was filtered to determine whether the actinide fraction was associated with particulate material or could be considered truly dissolved. Solution was passed sequentially through filters having pores ranging from 1.0 μm to 1 nm in diameter. The filters and the liquid that passed through each filter were analyzed for radionuclides. We then dissolved the filters, dried the resulting suspension, and exposed it to films sensitive to α particles to locate the source of α activity (*16, 17*). When α tracks were observed, the particles producing those tracks were identified and transferred to a transmission electron microscope (TEM) grid. The structure and composition of the radioactive particle were then determined (Figs. 1 and 2).

The radionuclide concentrations on the filters and in the liquid that passed through each filter were determined with α spectroscopy. The results of the tests (Table 1) indicate that 70% of the Np passed through all filter sizes; this fraction of Np can be considered truly dissolved. On the contrary, >99% of the Am and Pu was retained as colloidal solids. Additionally, results for test #1 were essentially unchanged on settling (Table 1). This suggests that the filtered material had accumulated in solution as suspended material and was stable in this form during the test period (39 weeks) and during an additional 6 weeks of settling. In these tests, most of the α radiation was due to the decay of ^{241}Am; however, in samples where ^{239}Pu was also detected, its behavior mirrored that of Am. Thus, we discuss Pu and Am release together.

Table 1. Masses of Np and (Pu + Am) in the unfiltered solution (top two rows) and the percent of the starting radioactivity after each pass through filters of decreasing pore size. Error in the absolute measurements is ~15% of the amount present. Absolute radioactivity levels in the test solutions differ between test #1 and test #2 because water flow patterns were different. Immediately upon termination of the tests, a small aliquot was removed with minimal disturbance of the solution (initial aliquot). For test #1, the solution was then stored at room temperature for 6 weeks. At that time, another aliquot was taken from the stagnant solution (delayed aliquot), and the remaining solution was filtered. For test #2, filtering was performed after removal of the initial aliquot.

Fraction	Np		Pu + Am	
	#1	#2	#1	#2
	(10^{-8} g)		*(10^{-10} g)*	
Initial	17.4	6.0	108	1087
Delayed	16.3		119	
	(Percent passage)			
1 μm	100	100	4	0.6
0.4 μm	100	100	4	0.6
0.1 μm	100	100	3	0.4
0.05 μm	85	100	2	0.3
0.015 μm	85	72	2	0.3
0.003 μm	70	70	1	0.01
0.001 μm	70	65	0.05	0.00

In general, the ratio of radioactivity of the filtered to the dissolved fraction was greater than 1000:1.

The compositions and mineralogy of the α-emitting particles on TEM grids were determined with analytical electron microscopy (AEM) (*18*). Compositional analyses were performed with x-ray energy-dispersive spectroscopy (EDS), and crystal structures were investigated with lattice fringe imaging and electron diffraction. A sample of colloid-containing residue was also analyzed by x-ray diffraction. The colloids are a matrix of clay that contains submicrometer inclusions (Fig. 2). The clay is an Fe- and Na-rich alumino silicate (with minor concentrations of Ca, Ti, and Ni) that has a basal lattice spacing of 10 to 12 Å. This basal spacing, combined with x-ray diffraction data, suggests that the clay is Na-rich smectite (*19*). The submicrometer inclusions contain mostly Ca, Th, P, and O, and minor amounts of U and Pb. Electron diffraction (Table 2) and x-ray diffraction data indicate that the inclusions are the mineral brockite [ideally $(Ca,Th)PO_4 \cdot H_2O$ (*20*)].

We compared the densities of the α tracks originating from brockite-rich versus clay-rich material to establish that the Am (and Pu) are carried in the brockite inclusions rather than the clay matrix. (Both Am and Pu are present at levels ≪0.1% by weight and are therefore undetectable by EDS.) Figure 1C shows tracks emanating from two colloid particles. Particle (i) is almost four times larger than particle (ii), but it produces only a third as many tracks as particle (ii). Bright-field and backscattered electron images (Fig. 1, A and B) and EDS analyses indicate that particle (i) is clay-rich, whereas particle (ii) is brockite-rich. Thus, the α activity and hence Am (and Pu) concentrations are associated with the brockite and not the clay.

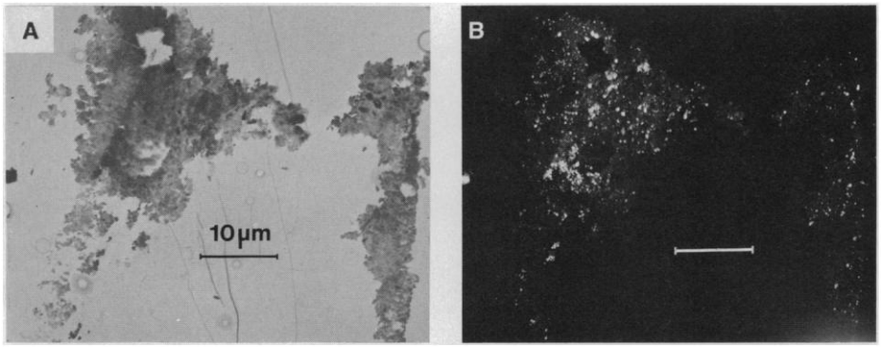

Fig. 2. (**A**) Bright-field electron micrograph of dispersed colloid residue supported on a thin (<20 nm thick) carbon film. The residue is a mixture of clay and brockite. (**B**) Corresponding backscattered electron image (10-μm scale bar). The bright spots reveal the positions of submicrometer brockite inclusions within the clay. The original material trapped on the filter with 1-μm-diameter pores had a size distribution only slightly larger than 1 μm and had to be crushed and dispersed to resolve the brockite.

Table 2. Measured electron diffraction parameters from a Pu- and Am-bearing inclusion compared to those of brockite [$(Ca,Th)PO_4 \cdot H_2O$].

Inclusion spacing (Å)*	Brockite spacing† (Å)
6.06	6.06
4.32	4.37
3.25	3.47
2.94	3.03
2.72	2.83
2.29	2.37
	2.15
2.05	1.92
	1.86
1.78	1.75
	1.69
1.65	1.67
	1.55
1.49	1.46
	1.35
	1.31

*±2.5% error. †From Fisher and Meyrowitz (*20*).

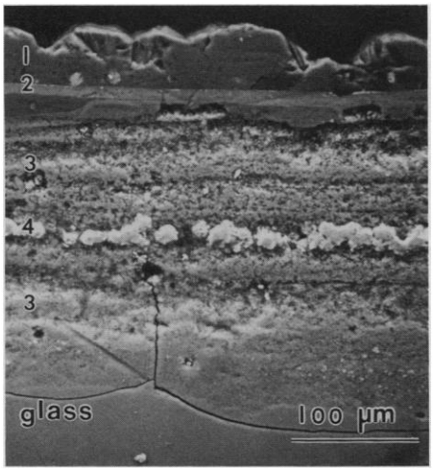

Fig. 3. Backscattered electron image of a cross section of glass exposed to water vapor. As the glass hydrates, elemental segregation occurs, secondary phases (1) form on the original surface (2) of the glass, and a hydrated layer (3) simultaneously penetrates the glass. Calcium, phosphorus, thorium, and other actinides redistribute within the hydrated layer to form discrete brockite inclusions (4) as small as 10 nm in diameter. Actinide redistribution preferentially concentrates Th, U, Pu, and Am from the glass in the inclusions, which are subsequently mobilized as colloids.

The Am- (and Pu-) bearing colloidal particles form by a mechanism distinct from those that form radiocolloids and pseudocolloids. Whereas radiocolloids and pseudocolloids develop from solution, the colloids studied here are fragments of a hydrated layer that spalled from the glass surface during aqueous alteration. This spallation mechanism can generate primary colloidal particles with elevated radionuclide levels. Whereas radiocolloids and pseudocolloids typically may be expected to incorporate only a small fraction of the actinide content of the waste (9), the radioactivity associated with primary colloids can be highly concentrated within specific actinide-rich compounds that form directly from the waste.

We examined the spallation mechanism of colloid formation by exposing a glass, of composition similar to that described above, to water vapor. Exposure to water vapor is known to accelerate glass reaction (*21*) and thus provides an ideal method to examine redistribution of elements during glass reaction. Water vapor is also likely to be more prevalent in the Yucca Mountain environment than liquid water. In the presence of water vapor, a thin film of water sorbs onto the glass surface, where it becomes concentrated in cations leached from the glass. Mineral phases nucleate from the film and form on the surface of the glass, and, at the same time, a hydrated or leached layer penetrates the glass (Fig. 3) (*22*). Because this layer is analogous to the hydrated layer that forms during the dripping water tests, its mineralogy should be similar to that of the primary colloids filtered from the ground water. Scanning electron microscopy (SEM) and AEM were used to study polished thick-flat and ultramicrotomed thin sections of the vapor-exposed specimen. Inclusions were identified that exhibited the same compositional and diffraction characteristics as the Pu- and Am-bearing inclusions in the colloids, and the clay in the hydrated layer was Na-rich smectite (Fig. 3). This correspondence in phases confirms that the reacted glass layer is the source of the primary colloidal particles.

These observations have several ramifications. First, because the majority of Np remained in solution, Np performance in the repository appears to be adequately treated with current assumptions of solubility-controlled transport. Second, because the Pu- and Am-bearing colloids are readily generated from reacted glass, transport of Pu and Am may be dominated by movement of these colloids. Thus, the EBS system should be designed to inhibit colloid transport in case of unexpected liquid water contact with the waste. Assessments of the ability of the environment near the repository to retard radionuclide transport should also consider colloid migration and trapping processes. Finally, a conservative performance assessment should be based on the identity and transport properties of specific actinide-bearing phases that result from waste form reaction. The colloid phases generated and their transport properties will likely vary, depending on the type of waste form (spent fuel or glass) and on the glass composition.

The approach taken in this study, that is, examination of radionuclide-bearing waste, combined with methods for identifying and characterizing submicrometer colloidal particles, also has applications to cleanup of sites contaminated with hazardous wastes (*23*). The identity of small radionuclide-bearing phases may help in determining transport rates, developing remediation methods, and supporting risk assessment studies.

REFERENCES AND NOTES

1. U.S. Department of Energy, "Draft mission plan amendment," *DOE/RW-0316P* (Office of Civilian Radioactive Waste Management, Washington, DC, 1991).
2. _____, "Site characterization plan: Yucca Mountain site, Nevada research and development area, Nevada," *DOE/RW-1099* (Office of Civilian Radioactive Waste Management, Washington, DC, 1988).
3. For the time period after 1000 years, Pu and Am will be the dominant radionuclides based on curie content of the waste. Resolution of their behavior must be established to predict repository performance. Compare V. Oversby, *Nucl. Chem. Waste Manage.* **7**, 149 (1987).
4. M. J. Apted and D. W. Engel, in *High-Level Radioactive Waste Management Proceedings* (American Nuclear Society, LaGrange Park, IL, 1990), vol. 1, pp. 388–393.
5. E. S. Patera, D. E. Hobart, A. Meijer, R. S. Rundberg, *J. Radioanal. Nucl. Chem. Artic.* **142**, 331 (1990).
6. H. Nitsche, *Radiochim. Acta* **52/53**, 3 (1991).
7. J. I. Kim, *ibid.*, p. 71.
8. Colloids are small particles that have peculiar properties in solution due to their high surface area to mass ratio. As our concern here is that material released from waste glass may remain suspended in solution and be subject to transport, we use the operational definition of a colloid rather than the classical size-based definition of ≤1 μm. In geologic systems, particles up to ~10 μm in diameter may behave as colloids. See R. Bates and J. Jackson, Eds., *Dictionary of Geological Terms* (American Geological Institute, Anchor, New York, 1976); S. Yariv and H. Cross, *Geochemistry of Colloid Systems* (Springer-Verlag, New York, 1979); W. Stumm, *Environ. Sci. Technol.* 11, 1066 (1977).
9. J. D. F. Ramsay, *Radiochim. Acta* **44/45**, 169 (1988).
10. M. B. ten Brink, D. L. Phinney, D. K. Smith, *Mater. Res. Soc. Symp. Proc.* **212**, 641 (1991).
11. J. K. Bates, W. L. Ebert, T. J. Gerding, in *High-Level Radioactive Waste Management Proceedings* (American Nuclear Society, LaGrange Park, IL, 1990), vol. 1, pp. 1095–1102.
12. T. A. Abrajano, J. K. Bates, A. B. Woodland, J. P. Bradley, W. L. Bourcier, *Clays Clay Miner.* **38**, 537 (1990).
13. J. K. Bates and T. J. Gerding, *Argonne National Laboratory Report ANL-89/24* (1990).
14. The glass composition (*15*) for major cations and actinides (element mass percent) is Al = 3.5, B = 2.8, Fe = 8.1, K = 2.8, Li = 1.3, Na = 7.8, P = 1.0, Si = 21.4, Am = 0.006, Np = 0.02, Pu = 0.07, Th = 2.9, and U = 0.5.
15. G. D. Maupin, W. M. Bowen, J. L. Daniel, *Pacific Northwest Laboratory Report PNL-5577-10* (1988).
16. We used a combination of particle micromanipulation procedures, autoradiography, and AEM to characterize the colloidal particles. A polycarbonate filter (including particles) with 1-μm-diameter pores was dissolved in chloroform, and the (colloid) residue that remained was dispersed within a thin (~1 μm thick) collodion film. The film was exposed to nuclear emulsion for up to 30 days. The photosensitive emulsion was developed, and the positions and orientations of nuclear tracks (in the emulsion) relative to specific colloidal particles (in the collodion) were recorded. The collodion film was then mounted on a carbon-coated TEM grid, and the collodion was dissolved. By preserving the relative positions of colloidal particles during transfer onto a TEM grid, it was possible to locate and analyze particles responsible for specific tracks in the emulsion (Fig. 1).
17. J. P. Bradley and D. E. Brownlee, in *Microbeam Analysis*, R. Gooley, Ed. (San Francisco Press, San Francisco, 1983), p. 187; A. Teetsov and J. P. Bradley, *Lunar Planet Sci.* **XVII**, 883 (1986).
18. Analyses were performed on (200-keV) JEOL 2000FX analytical electron microscopes equipped with Tracor Northern energy-dispersive spectrometers and Gatan (parallel detector) energy electron loss spectrometers.
19. G. W. Brindley, in *Crystal Structure of Clay Minerals and Their X-ray Identification*, G. W. Brindley and G. Brown, Eds. (Mineralogical Society, London, 1984), p. 125.
20. J. L. Fisher and D. S. Meyrowitz, *Am. Mineral.* **47**, 1364 (1962).
21. J. K. Bates, L. J. Jardine, M. J. Steindler, *Science* **218**, 51 (1982).
22. W. L. Ebert, J. K. Bates, W. L. Bourcier, *Waste Manage.* **11**, 205 (1991).
23. J. F. McCarthy and J. M. Zachara, *Environ. Sci. Technol.* **23**, 496 (1989).

24. Supported by the U.S. Department of Energy, Office of Civilian Radioactive Waste Management, Yucca Mountain Site Characterization Project, under subcontract to Lawrence Livermore National Laboratory, SANL-110-003.

28 October 1991; accepted 11 February 1992